JOURNAL OF CATALYSIS 128, 113–125 (1991)

Reactive Lattice Oxygen Sites for C_4–Hydrocarbon Selective Oxidation Over β-$VOPO_4$

M. E. LASHIER AND G. L. SCHRADER*

Department of Chemical Engineering and Ames Laboratory—U.S.D.O.E., Iowa State University, Ames, Iowa 50011

Received January 16, 1990; revised August 8, 1990

The role of lattice oxygen species in the catalytic oxidation of *n*-butane to maleic anhydride has been investigated using β-$VOPO_4$ labeled with ^{18}O. The catalyst was prepared by stoichiometric reaction of $(VO)_2P_2O_7$ with $^{18}O_2$ using solid state preparation techniques. The β-$VOPO_{7/2}$ $^{18}O_{1/2}$ was characterized using laser Raman and Fourier transform infrared spectroscopies: preferential incorporation at P–O–V sites was observed. A pulse reactor was used to react *n*-butane, 1-butene, 1,3-butadiene, furan, γ-butyrolactone, and maleic anhydride with the catalyst in the absence of gas-phase O_2. Incorporation of ^{18}O into the products was monitored by mass spectrometry. Specific lattice oxygen sites could be associated with the reaction pathways for selective or nonselective oxidation. The results of this study also indicate that the initial interaction of *n*-butane with β-$VOPO_4$ is fundamentally different from the initial interaction of olefins or oxygenated species. The approach used in this research—referred to as Isotopic Reactive-Site Mapping—is a potentially powerful method for probing the reactive lattice sites of other selective oxidation catalysts.

INTRODUCTION

Transformation of relatively cheap—but rather inert—paraffins to valuable chemical intermediates has become attractive industrially. The selective oxidation of *n*-butane to maleic anhydride is one of the few large-scale commercial processes currently utilizing this type of chemistry. The key to this processing technology is the existence of highly active and selective vanadium–phosphorus–oxide (V–P–O) catalysts. Although a wide variety of V–P–O phases has been discussed in the literature, phases such as $(VO)_2P_2O_7$ and β-$VOPO_4$ have been extensively investigated (*1–3*). Of particular interest have been the structure, stability, and oxidation-reduction characteristics of the catalysts (*4*).

Activation of *n*-butane over V–P–O catalysts appears to occur in a very specific manner (*5*). While the initial activation of the paraffin via hydrogen abstraction is a crucial function of these catalysts, it is only the first step of a complicated reaction pathway. Additional hydrogen atoms must be abstracted, while three oxygen atoms must be inserted to finally produce maleic anhydride. Several mechanisms have been proposed for the selective oxidation route to maleic anhydride (*5–16*), the most common being *n*-butane → 1-butene → 1,3-butadiene → furan → maleic anhydride (*17–21*). Centi and Trifiro (*5*) proposed a more complex mechanism for which the major pathway to maleic anhydride can be summarized as *n*-butane → 1-butene → 1,3-butadiene → dihydrofuran → furan → maleic anhydride. The specific catalytic sites involved in these reactions steps have yet to be identified. In addition, nonselective reaction pathways which produce CO_2 and H_2O exist; the sites

* To whom correspondence should be addressed.

0021-9517/91 $3.00

or adsorbed species involved in these conversion also have not been conclusively determined.

The role of lattice oxygen in the reaction of *n*-butane with V–P–O catalysts has been examined by several workers. Kruchinin *et al.* (*22*) have demonstrated that lattice oxygen is involved in the production of CO, CO_2, and maleic anhydride. This was accomplished by following the incorporation of ^{18}O from the gas phase into the products in a closed recirculating system. The ^{18}O incorporation was gradual, indicating that oxygen from the lattice was being directly used to produce these products; oxygen uptake from the gas phase into the lattice was also shown to occur. A Mars–van Krevelen mechanism in which the catalyst sequentially undergoes reduction and oxidation steps was believed to be appropriate. Pepera *et al.* (*23*) have made a similar observation, but they believe that the oxidation and reduction is limited to the near surface layers of the catalyst. In their studies, the surface of $(VO)_2P_2O_7$ was equilibrated with ^{18}O and reacted with *n*-butane; the incorporation of ^{18}O into CO_2 was monitored. On the basis of their observations and the consideration of several reactions models, they concluded that surface oxygen is in rapid equilibrium with the gas phase (although no isotopic scrambling was observed).

Additional studies (*18, 23–28*) have also investigated the importance of lattice oxygen in the oxidation of *n*-butane to maleic anhydride. Work by Gleaves *et al.* (*29*) has suggested that both lattice and surface activated (adsorbed) oxygen are involved in the complete reaction mechanism. On the basis of experiments involving small pulses of reactants fed to a catalyst be held at high vacuum, a highly mobile—yet irreversibly adsorbed—oxygen species was believed to be responsible for *n*-butane activation and the oxidation of furan to maleic anhydride. This species was thought to be formed by strong chemisorption of an electrophilic dioxygen molecule at a V(+5) site. Intermediate oxidation steps (1-butene to furan) apparently involve lattice oxygen at the surface, specifically allylic oxydehydrogenation and oxygen insertion leading to ring closure to form furan. Two sources of oxygen were believed to exist for the formation of CO_2: a "fast" source identified as a highly reactive chemisorbed oxygen and a "slow" source attributed to lattice oxygen. Centi (*2*) *et al.* also suggested that CO_2 can be formed from an adsorbed dioxygen molecule, based on the blocking of oxygen adsorption sites by NH_3.

Although the experiments conducted by Gleaves *et al.* (*29*) indicate that a strongly adsorbed oxygen species is responsible for *n*-butane activation, several researchers claim that weakly adsorbed oxygen species or oxygen atoms at defect sites are responsible (*24, 30, 31*). Other work has indicated that weakly adsorbed, activated oxygen is very electrophilic and produces nonselective cracking (*32, 33*). Centi and Trifiro (*34*) ascribe weakly electrophilic sites to V=O species. They postulate that V(+5)=O is responsible for oxygen insertion, while V(+4)=O or V(+4)–O–P sites are responsible for hydrogen abstraction.

In a previous report (*35*) we have described a technique which permits the different reactivities of lattice oxygen in β-$VOPO_4$ to be examined. In this method, which we refer to as Isotopic Reactive-Site Mapping (IR-SM), ^{18}O is incorporated in specific oxygen lattice sites through solid state synthesis or surface-reduction techniques. The location of the ^{18}O is then determined using spectroscopic techniques. Finally, the labeled catalyst is reacted with hydrocarbons, for example, in a pulse reactor and in the absence of gas phase oxygen; the products are monitored by mass spectrometry to determine the uptake of ^{18}O into specific products. Our previous work (*35*) focused on studies of ^{18}O incorporation into maleic anhydride or CO_2 using *n*-butane feeds. In the research reported here, these results have been extended to other hydrocarbon feeds which may be possible intermediates in the conversion of *n*-butane to maleic anhydride. New information concerning the role of spe-

cific lattice oxygen sites in the reaction pathway has been provided.

EXPERIMENTAL PROCEDURE

Synthesis of ^{18}O-Enriched β-$VOPO_4$

^{18}O-enriched β-$VOPO_4$ was prepared by the solid state reaction of $(VO)_2P_2O_7$ with $^{18}O_2$. Synthesis of the $(VO)_2P_2O_7$ material has been described previously (*6*). $^{18}O_2$ obtained from Merck, Sharp, and Dohme had an isotopic enrichment of 97.8%. Powdered $(VO)_2P_2O_7$ (0.50 g) was charged to a 9-mm-o.d. Pyrex tube which could be evacuated and back-filled with a stoichiometric quantity of $^{18}O_2$. The reaction tube was heated at 823 K for 24 h followed by cooling to 473 K at a rate of 50 K/h. (This method was also used to prepare β-$VOPO_4$ using $^{16}O_2$.)

Catalyst Characterization and Location of ^{18}O Incorporation

X-ray diffraction, laser Raman spectroscopy, and Fourier transform infrared spectroscopy were used to characterize all catalyst materials (*6*). All fresh catalysts were single-phase materials.

Characterization of the ^{18}O-enriched β-$VOPO_4$ by laser Raman and Fourier transform infrared spectroscopies revealed band shifts due to the incorporation of the isotopic label. The Raman spectra were obtained with a Spex 1403 spectrometer using the 514.3-nm line of a Spectra Physics Model 2020-05 argon ion laser (100 mW at the source). A Nicolet 1180E computer system was used to accumulate 50 scans at 2 cm^{-1} resolution with a scanning rate of 3.25 cm^{-1}/s; peak intensities were integrated using a curve fitting routine available from Nicolet. The infrared spectra were obtained using a Nicolet 60SX Fourier transform infrared spectrometer. Data were obtained using KBr pellets; 2 cm^{-1} resolution and accumulations of 200 scans were employed.

Reactor Studies and Mass Spectrometry of Oxidation Products

Reactions of *n*-butane, 1-butene, 1,3-butadiene, furan, γ-butyrolactone, and maleic anhydride using the ^{18}O-enriched catalyst were performed in a pulse-reactor system (*36*). The reactor was constructed from a passivated 1/4 in stainless steel tube. For each experiment, 0.2 g of catalyst was pressed, crushed, and sieved to 10–20 mesh before use in each experiment. After loading the catalyst, the reactor was purged with a helium flow of 50 cm^3/min for 3 h and then was heated from room temperature to the reaction temperature (773 K for *n*-butane and 723 K for other feeds). This temperature was maintained for 1 h. Pulse studies were performed at a rate of about 1 pulse per minute for a total of at least 75 pulses. A 10-port Valco valve equipped with 0.5-ml injection loops was used to introduce the hydrocarbon pulses. The valve and injection loops were maintained at 425 K.

The gas compositions were regulated by Tylan mass flow controllers (Model FC260). *n*-Butane, 1-butene, and 1,3-butadiene (Matheson, instrument grade) were diluted with helium (Matheson, zero grade) to a hydrocarbon content of 2%. To provide low (less than 1%) concentrations of furan (Kodak), γ-butyrolactone (Alfa), and maleic anhydride (Kodak), helium was fed to a saturator (*36*) maintained at temperatures corresponding to vapor pressures of less than 10 torr for each species. For the furan studies, the saturator was placed in a dry ice/acetone bath which was maintained at 195 K to provide a furan vapor pressure of about 1 torr (about 0.1 mol%). For the γ-butyrolactone studies, a feed of about 1% hydrocarbon could be produced by maintaining the saturator at 330 K. A saturator temperature of 340 K was maintained for maleic anhydride, which also produced a concentration of slightly less than 1% hydrocarbon.

Mass spectrometry was performed using a UTI 100C precision quadrupole mass analyzer controlled by a PDP 11/23 computer. The mass analyzer was interfaced with the microreactor system by a glass SGE single-stage molecular jet separator. The amount of ^{18}O in maleic anhydride, CO_2, furan, and

TABLE 1

Mass Spectral Ranges Scanned Every Fifth Pulse and Species of Interest in Those Ranges

Range (*m/e*)	Species	Number of mass spectrometer scans/pulse
42–50	CO_2	80
17–22	H_2O	80
67–90	Furan and γ-butyrolactone	20
95–110	Maleic anhydride	30
50–60	*n*-butane, 1-butene, 1,3-butadiene	40

γ-butryolactone was determined for the oxidation of *n*-butane, 1-butene, 1,3-butadiene, furan, γ-butyrolactone, and maleic anhydride. Because the experiments were conducted in the pulse mode, it was not possible to accurately monitor the entire mass spectral region of interest (40–110 *m/e*). Therefore, the mass spectrum was divided into five ranges that could be monitored for each pulse (Table 1). The entire spectral range was examined, however, using an unlabeled catalyst to ensure that all species were properly monitored. Any interferences (spectral overlaps) between species in the mass-to-charge ratios (*m/e*) were compensated for in the final calculations.

In this work, the amount of ^{18}O present in each species is expressed as a percentage of the total oxygen present. The amount of ^{18}O in maleic anhydride is expressed as

$$\frac{\Sigma I_{100} + 2\Sigma I_{102} + 3\Sigma I_{104}}{3(\Sigma I_{98} + \Sigma I_{100} + \Sigma I_{104})}$$

where I is the intensity of the indicated *m/e* peak. For 1-butene and 1,3-butadiene feeds, phthalic anhydride was formed, and the peak intensity at *m/e* 104 was corrected. The amount of ^{18}O present in furan is expressed as

$$\frac{\Sigma I_{70}}{\Sigma I_{68} + \Sigma I_{70}}.$$

Corrections were made for interference at *m/e* 70 from a minor maleic anhydride fragment. The amount of ^{18}O in CO_2 is expressed as

$$\frac{\Sigma I_{44} + 2\Sigma I_{48}}{2(\Sigma I_{44} + \Sigma I_{46} + \Sigma I_{48})}.$$

Corrections were made by subtracting the minor interferences at *m/e* 44 from *n*-butane and background CO_2. Low levels of CO could also be observed, but the data were significantly obscured by interference from background N_2 and $C^{16}O$.

EXPERIMENTAL RESULTS

Catalyst Synthesis and Location of ^{18}O-Labeled Sites

In Fig. 1 and Table 4, the Raman spectrum of ^{18}O-enriched β-$VOPO_4$ prepared by the solid state reaction of $(VO)_2P_2O_7$ with $^{18}O_2$ is compared to the Raman spectrum of β-$VOPO_4$ prepared in a similar manner using $^{16}O_2$. New bands decreased in intensity or were slightly broader for the ^{18}O-labeled sample. ^{18}O incorporation could be observed in a band appearing at 886 cm^{-1}; the ^{16}O band at 896 cm^{-1} had a similar intensity. Another weak band revealing ^{18}O incorporation was observed at 961 cm^{-1}. The intensity of this band, however, was only about 5% that of the corresponding band at 987 cm^{-1}; correspondingly, the intensity of the 987 cm^{-1} band was slightly reduced. The band at 998 cm^{-1} showed very little difference in intensity between the two catalysts. Only a very slight broadening of the band at 1072 cm^{-1} could be observed for the ^{18}O-labeled sample. A very small amount of unreacted $(VO)_2P_2O_7$ was indicated by an extremely weak band at 923 cm^{-1} in the spectrum of ^{18}O-enriched β-$VOPO_4$. Reaction of $(VO)_2P_2O_7$ with $^{16}O_2$ also produced β-$VOPO_4$ containing a very small amount of unreacted $(VO)_2P_2O_7$. (However, both of these bands cannot be seen clearly unless the intensity scale in Fig. 1 is expanded.) Only very slight changes occurred in the Raman spectrum of ^{18}O-enriched β-$VOPO_4$

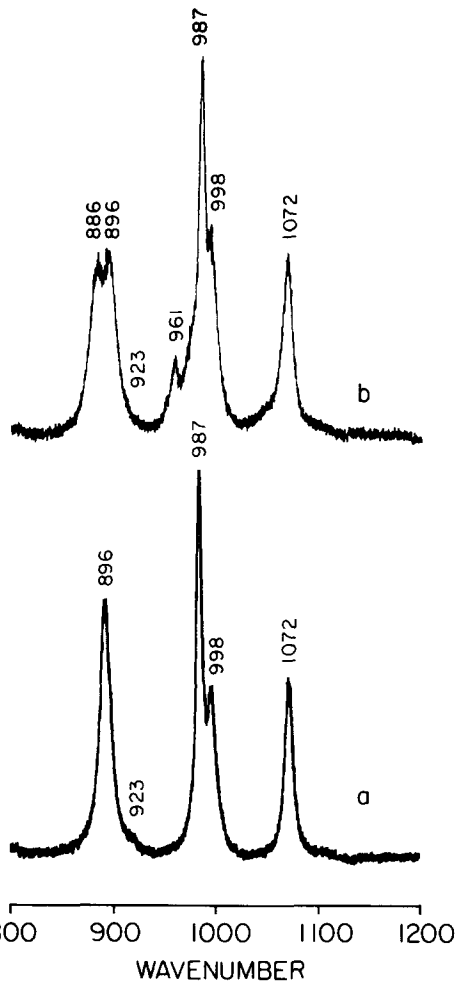

FIG. 1. Laser Raman spectra of (a) β-$VOPO_4$ and (b) ^{18}O-enriched β-$VOPO_4$.

after reaction with hydrocarbons (up to 100 pulses). The amount of $(VO)_2P_2O_7$ increased very little, and the overall intensity of the spectra decreased slightly.

The infrared spectra of the labeled and unlabeled catalysts are shown in Fig. 2. The characteristically broader band structure which is observed with infrared techniques makes identification of the band shifts somewhat less precise and intensity comparisons very difficult. Two bands at 998 and 1055 cm^{-1} do not appear to be altered by the incorporation of ^{18}O. However, the 952-cm^{-1} band position is shifted to 942 cm^{-1}. Another band appears at 962 cm^{-1}; the unlabeled catalyst also has some broad band structure present in this region (near 974 cm^{-1}). The appearance of the band at 962 cm^{-1} for the ^{18}O-labeled catalyst may correlate with the reduced intensity in this region. Quantification of the infrared peak intensities was not attempted.

Pulse Reactor/Mass Spectrometry Results

Relative product concentrations. Maleic anhydride, furan, and CO_2 were produced from all C_4–hydrocarbon pulses. Representative data are shown in Table 2, although there were variations in the amounts of products produced during a series of pulses. These differences are noted in the following discussion.

n-Butane produced smaller amounts of each product than most other feeds. The olefins were much more reactive, producing large amounts of maleic anhydride. 1-Butene pulses produced over 30 times as much maleic anhydride, 5 times as much furan,

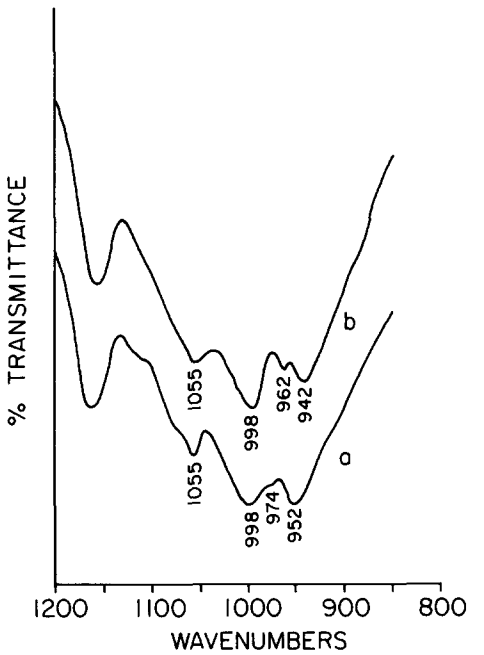

FIG. 2. Fourier transform infrared spectra of (a) β-$VOPO_4$ and (b) ^{18}O-enriched β-$VOPO_4$.

TABLE 2

Summary of the Relative Concentration (Per Pulse) of Products from Various Feeds

Feeds	Products		
	Maleic anhydride	Furan	CO_2
n-Butane	1	1	1
1-Butene	5	30	20
1,3-Butadiene	100	30	30
Furan	2	f[a]	4
γ-Butyrolactone	2	1	10
Maleic anhydride	f	0.1	10

[a] f = feed.

Note. The concentrations for each product are normalized to the corresponding level produced by *n*-butane. Variations depending on pulse number are described in the text.

and 20 times as much CO_2 per pulse as did *n*-butane. Maleic anhydride and CO_2 production decreased 90% from pulse 1 to pulse 75 for 1-butene, while furan production remained constant throughout the experiment. After about 5 pulses, phthalic anhydride could be detected. Maleic anhydride, furan, CO_2, and phthalic anhydride were produced from all 1,3-butadiene pulses. 1,3-Butadiene pulses produced over 30 times as much maleic anhydride, 100 times as much furan, and over 30 times as much CO_2 per pulse as did *n*-butane. From pulse 1 to pulse 75, the production of maleic anhydride decreased 95%, the production of CO_2 decreased 80%, and the production of furan remained unchanged.

Maleic anhydride and CO_2 were produced from nearly all furan pulses. Maleic anhydride was not detected in the first furan pulse, but from pulse 2 to pulse 75, the production level increased markedly. Eventually, furan pulses produced 2 times as much maleic anhydride and 4 times as much CO_2 per pulse as did *n*-butane. The CO_2 production per pulse remained nearly constant.

Maleic anhydride, furan, and CO_2 were produced from all pulses of γ-butyrolactone. The level of maleic anhydride production initially was very low, but the amount increased to a final level which was approximately 2 times that produced from *n*-butane. CO_2 was produced at a level 10 times greater than that produced from *n*-butane. The production of CO_2, however, decreased by 50% from pulse 1 to pulse 75. Initially, furan was produced from γ-butyrolactone at very low levels, but the production eventually increased to the same level observed from *n*-butane.

Furan and CO_2 were produced from all maleic anhydride pulses. Maleic anhydride pulses produced furan at about $\frac{1}{10}$ the level produced from *n*-butane while CO_2 was produced at about 10 times the corresponding level.

^{18}O incorporation into products. Representative data for the incorporation of ^{18}O into specific products are summarized in Table 3. In most cases, the level of ^{18}O incorporation was nearly constant. Some variation was observed for 1-butene, furan, and maleic anhydride feeds, but the effects were very small. No oxygen exchange was observed to occur between furan and the catalyst. Maleic anhydride fed to the reactor did undergo some oxygen exchange. The 5% ^{18}O incorporation did not change when the partial pressure of the maleic anhydride feed was reduced by about 30%.

DISCUSSION

Incorporation and Spectroscopic Location of ^{18}O Sites

The structure of β-$VOPO_4$ (Fig. 3) consists of VO_6 groups, frequently referred to as irregular octahedra (although reference to a pyramidal arrangement is also used), which form corner-sharing chains through V=O–V bonding (*37*); these chains are arranged to form sheets. The PO_4 tetrahedra share oxygen atoms with four VO_6 octahedra are bridged by corner sharing of oxygen between the PO_4 groups in one sheet with VO_6 groups in the next sheet; these oxygen atoms are involved in P–O–V bonding. The PO_4 tetrahedra also share corners with two octahedra in the same octahedral chain. These latter two oxygen atoms are crystallo-

TABLE 3

Summary of ^{18}O Content in All Products for Each Species Fed to β-$VOPO_{7/2}$ $^{18}O_{1/2}$ in the Absence of Gas Phase Oxygen

	Maleic anhydride (%)	Furan (%)	CO_2 (%)	γ-Butyrolactone (%)
n-Butane	12	28	5	np[a]
1-Butene	14	13	10	np
1,3-Butadiene	14	13	9	np
Furan	10	0	7	np
γ-Butyrolactone	12	22	5	3
Maleic anhydride	5	14	1	np

[a] np = (unlabeled and labeled) product not produced at detectable levels.

graphically distinct because of the displacement of the vanadium atoms from the center of the irregular octahedra. These oxygen atoms are also involved in P–O–V bonding. As shown in Fig. 3, these oxygen species can be considered to be in the equatorial plane of the VO_6 octahedra.

The synthesis of the ^{18}O-labeled β-$VOPO_4$ was based on the solid state reaction

$$(VO)_2P_2O_7 + \tfrac{1}{2}\,{}^{18}O_2 \rightarrow 2\ \beta\text{-}VOPO_{7/2}\ {}^{18}O_{1/2}.$$

This conversion route has been established previously using $^{16}O_2$ in flow systems (*38–39*) and in sealed-tube syntheses (*36*). The temperatures used in the syntheses reported in this research were lower than those examined by Bordes and co-workers (*39*), although the *in situ* Raman studies of Moser and Schrader (*38*) indicated that significant conversion to β-$VOPO_4$ occurs in a few hours at 550°C. A minimal loss of surface area occurred at the lower temperature. The reactants were used in stoichiometric proportion as determined by solid [$(VO)_2P_2O_7$] weight and gas ($^{18}O_2$) volume, and the extent of conversion could be monitored using Raman spectroscopy. For some samples, a very small amount of $(VO)_2P_2O_7$ was observable by an extremely weak band present at about 923 cm^{-1}. The extent of conversion observed by this method was independent of whether $^{18}O_2$ or $^{16}O_2$ was used.

The vibrational spectra of β-$VOPO_4$ has been reported by several research groups, and discussions of the band assignments have been provided by Bhargava and Condrate (*40*) and Moser and Schrader (*6*). In their early study, Bhargava and Condrate reported that a group factor analysis predicted that 42 bands should be active in the Raman spectrum and 31 bands should be active in the infrared spectrum. Since the β-$VOPO_4$ crystal is centrosymmetric, no coincidences should occur for the Raman and infrared data. Bhargava and Condrate reported the observation of 21 Raman bands and 11 infrared bands. Although Bhargava and Condrate mentioned the group factor approach, they presented an empirical assignment of a few bands on the basis of spectra of other orthophosphate or related compounds. By using this analogous spectral data, bands could be associated with "vanadium–oxygen" or "phosphorus–oxygen" bonds. However, it is

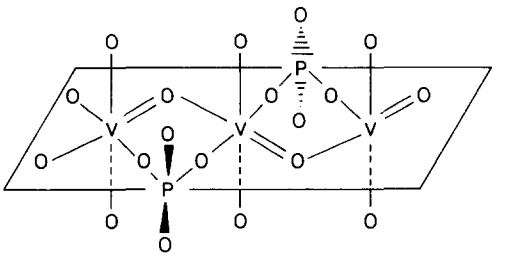

FIG. 3. Structure of β-$VOPO_4$.

clear that the structure of β-$VOPO_4$ is more complex than this notation would imply. For example, P–O–V bonding (rather than P–O bonds) are present in the structure as shown in Fig. 3. In considering generally vibrational spectroscopy of the solid state, it is recognized that there are many cases for which an assumption that the atomic groups (or polyhedra) associated with nearest neighbor bonding environments (from which the solid state structure may be constructed) vibrate independently of each other is invalid. For example Tarte (*41*) has demonstrated that this condition is fulfilled only under very special circumstances for spinels. Ross (*42*) has pointed out that if the vibrational frequencies of polyhedra around particular atoms are similar in magnitude, the interactions between the groups are probably comparable to those within groups; thus, the assignment of separate sets of vibrations as being characteristic of the distinct polyhedra (as in an approximation which would describe the spectra in terms of PO_4^{3-} groups) becomes meaningless. Only in cases of radically different bonding is it possible to make more specific assignments. These observations have also been made by Turrell (*43*), Nakamoto (*44*), and Wilkinson (*45*). Bhargava and Condrate (*40*) apparently recognized this in their mention of a group factor approach, but they clearly have chosen only an empirical description (a site group approach) in their brief summary of the observed bands.

In considering the region of the vibrational spectra reported here for β-$VOPO_4$, the insertion of ^{18}O has different effects on specific bands. Because of the distinct nature of the bonding, the Raman and infrared bands at 998 cm^{-1} have been assigned to the covalent bond V=O; spectral studies of V_2O_5 and other metal orthophosphates stongly support this conclusion ((*40*) and references within). No ^{18}O would appear to be incorporated at these sites because of the lack of intensity changes or shifts in either vibrational spectra. The other vibrational bands must be associated with P–O–V bonding. The Raman band at 1072 cm^{-1} appears to be unaffected by the insertion of ^{18}O while other bands at 987 cm^{-1} (some reduction in intensity, new band at 961 cm^{-1}) and 896 cm^{-1} (reduced in intensity, new band at 886 cm^{-1}) clearly are. Similar behavior is observed for the infrared bands at 1055 cm^{-1} (unchanged), 974 cm^{-1} (shifted to 962 cm^{-1}), and 952 cm^{-1} (shifted to 942 cm^{-1}). As discussed earlier, the structure of β-$VOPO_4$ involves three P–O–V bond distances. The spectra would indicate that ^{18}O is incorporated preferentially at one P–O–V site, with a smaller amount of ^{18}O present at another P–O–V site. The other P–O–V site appears to incorporate no ^{18}O.

The ^{18}O incorporation, in general, could have proceeded otherwise: random distribution of ^{18}O in the lattice could have occurred or complete incorporation of ^{18}O into all oxygen sites for a limited portion or region of the catalyst might have happened. However, the Raman and infrared characterization show that these eventualities did not occur.

Selective and Nonselective Oxidation Pathways

By considering the reactor results combined with the spectroscopic knowledge of the nature of the ^{18}O incorporation, it is possible first to develop a better understanding of the sites that are involved in partial oxidation (production of maleic anhydride) versus complete combustion (production of CO_2). The oxidation of *n*-butane by ^{18}O-labeled β-$VOPO_4$ resulted in the preferential incorporation of ^{18}O into maleic anhydride as compared to CO_2. The ^{18}O content of maleic anhydride was more than two times greater than that for CO_2; a relatively high level of ^{18}O incorporation into maleic anhydride was also observed for 1-butene reactions. For both feeds, the ^{18}O content of maleic anhydride was nearly 12–14% ^{18}O. To account for this selective incorporation, a "pool" of oxygen containing about 13% ^{18}O must exist. If all oxygen atoms associated with P–O–V bonding were closely similar in re-

TABLE 4

Effect of ^{18}O Incorporation on Laser Raman Peak Intensities for β-$VOPO_{7/2}$ $^{18}O_{1/2}$

Band Position		Assignment	^{18}O peak intensity/ total ^{16}O and ^{18}O peak intensity (%)
^{16}O band (cm^{-1})	^{18}O band (cm^{-1})		
1072	—	P—O—V_a	0
998	—	V=O	0
987	961	P—O—V^b	5
896	886	P—O—V^b	40

[a] Two sites per PO_4 group.
[b] One site per PO_4 group.

activity, such a source of ^{18}O would exist, based on the intensities of the Raman bands (four P–O–V sites with the ^{18}O incorporation as shown in Table 4). This equivalence in reactivity may be enhanced if these sites become more structurally similar at the catalyst surface than in the catalyst bulk.

The ^{18}O levels found in CO_2 indicate that total oxidation products are likely produced by more than one route. One pathway–the combustion of maleic anhydride to CO_2—has been shown to occur over β-$VOPO_4$ (*46*). CO_2 produced from maleic anhydride contains only about 1% ^{18}O. Clearly, most reactions must occur at unlabeled sites, such as the highly reactive V=O sites needed for combustion of the relatively stable maleic anhydride. CO_2 produced from *n*-butane and other hydrocarbon feeds (examined as possible intermediates) has a considerably higher level of ^{18}O; this indicates that direct combustion of these hydrocarbons must also proceed (*35*). A possible mechanism would involve electrophilic attack at the carbon–carbon bonds of *n*-butane and/or other hydrocarbon intermediates at V=O sites. These sites have been previously identified as being electrophilic by Garbassi *et al.* (*47*). The "cracking" reactions which would proceed at these sites would produce highly reactive C_1–C_3 species capable of interacting with all available oxygen sites to produce CO_2. If complete combustion proceeded exclusively on the V=O sites, the amount of ^{18}O in CO_2 would be low since the Raman spectra indicate that no ^{18}O is incorporated at these sites. On the other hand, if combustion occurred at all P–O–V sites, an ^{18}O level of 13% would be observed. If the C_1–C_3 species were sufficiently reactive to interact with all oxygen sites in the catalyst, an ^{18}O level of 10% would be observed. These levels are approached for 1-butene and 1,3-butadiene, probably due to the greater reactivity of these feeds. The lower level of ^{18}O incorporated into CO_2 from *n*-butane (5%) is probably also related to the lower reactivity of this feed.

Mechanistic Implications

It was also possible to relate the production of partially oxygenated intermediates with the reactivity of specific oxygen sites. The use of a pulse reactor was attractive since the transient nature of the pulse experiment allowed possible intermediates to be detected; the effects of catalyst reduction and deactivation could also be minimized. The latter may be especially important when one is operating in the absence of gas-phase O_2. Less than 1% of the available surface oxygen was consumed per pulse in the experiments conducted in this study. It is interesting, however, that most of the results reported in this study were consistent with those previously reported in the continuous flow experiments (*35*).

A comparison of the ^{18}O content of furan produced from *n*-butane reveals that the activation of the paraffin produces an adsorbed intermediate which undergoes oxygen incorporation only at some lattice sites to produce an adsorbed furan-like species. Small amounts of this species desorb as gas-phase furan under the conditions of these experiments, and the ^{18}O content is very high (28% ^{18}O). Clearly, a pool of oxygen with a high content of ^{18}O would be required. Both the laser Raman and the infrared char-

acterization indicate that such a concentration of ^{18}O could exist. For example, ^{18}O incorporation affects the band at 896 cm^{-1} most dramatically (a 40% change in intensity). In comparison the ^{18}O levels observed in furan formed from 1-butene and 1,3-butadiene were much lower (13%). This indicates that furan produced from these feeds is formed through a less specific interaction, likely involving the range of P–O–V sites. This is due in part to the greater reactivity of 1-butene and 1,3-butadiene; clearly, both of these feeds produce much furan, as shown in Table 2.

It should be pointed out that no gas-phase olefins were observed when *n*-butane was fed to the reactor. In general, if such olefins are produced during *n*-butane oxidation, they can be detected as desorption products only by using special low-pressure reactor environments (*29*) or by using low-surface-area, low-activity phases (*6*). Therefore, "free" olefins are not likely intermediates for *n*-butane oxidation; the dehydrogenated surface species derived from *n*-butane are apparently rather tightly bound. These surface-constrained species could be expected to react with specific oxygen sites in a much different manner than gas-phase olefins. The nature of the ^{18}O incorporation into intermediates formed from *n*-butane is, thus, strongly influenced by the fact that the intermediates are strongly adsorbed. Gas-phase 1-butene and 1,3-butadiene can react with a broader range of oxygen sites.

The ^{18}O content of maleic anhydride formed from *n*-butane, 1-butene, and 1,3-butadiene provides further mechanistic information about the next mechanistic step which is frequently proposed: conversion of the adsorbed furan-like species to maleic anhydride. As mentioned previously, for *n*-butane feeds the furan-like intermediate contains about 28% ^{18}O. To produce maleic anhydride containing 12% ^{18}O, additional oxygen atoms would have to be derived from sites containing approximately 5% ^{18}O. The Raman spectra indicate that there are sites with relatively low amounts of ^{18}O (the 987 and 961 cm^{-1} related bands). 1-Butene and 1,3-butadiene produce maleic anhydride with a slightly higher level of ^{18}O (14%). The conversion of these hydrocarbons to maleic anhydride would appear to involve the addition of oxygen from all P–O–V sites. Since both 1-butene and 1,3-butadiene produce considerable amounts of furan in the reactor effluent, it would be expected that the incorporation of ^{18}O into maleic anhydride would be more similar to results for furan feeds, as discussed next.

As for the case of olefin intermediates, it is likely that furan present in the gas phase (free furan) may adsorb and react at different sites than does an adsorbed furan-like species produced from the oxidation of *n*-butane. Furan is certainly more reactive than *n*-butane with respect to both maleic anhydride and CO_2 production (although it is much less reactive than the olefins). The levels of ^{18}O incorporation into maleic anhydride formed from a furan feed are near 10%; this is lower than the 12% for *n*-butane or the 14% observed from the olefins. Only two oxygen atoms must be added to produce maleic anhydride from furan, and oxygen exchange was not observed to occur for furan. A pool of oxygen involving 13% ^{18}O appears to be utilized, again similar to the sites suggested to be involved in the conversion of furan produced from 1-butene and 1,3-butadiene. Free furan is more likely to be an intermediate for olefin oxidation than *n*-butane conversion to maleic anhydride.

The products from γ-butyrolactone feeds were unusual since it was observed that both addition of oxygen to form maleic anhydride and loss of oxygen to form furan occurred. At the same time, only small amounts (3%) of the oxygen in γ-butyrolactone in the reactor effluent underwent oxygen exchange. The ^{18}O content of the maleic anhydride was 12%. If it is presumed that the lactone is directly converted to the anhydride by the addition of oxygen, then the main source of this oxygen must contain a large amount of ^{18}O (it is possible that some oxygen insertion occurs also from other sites since the ^{18}O

content of maleic anhydride is slightly low). The ^{18}O content of furan produced from γ-butyrolactone is remarkably high (22%). Clearly, the exchange mechanism is unlikely to produce these high levels of ^{18}O; therefore, it is likely that γ-butyrolactone must undergo a loss of all oxygen before adding oxygen at sites involving high levels of ^{18}O.

Maleic anhydride detected in the reactor effluent when maleic anhydride pulses were fed contained low levels of ^{18}O (5%), indicating that an oxygen exchange mechanism exists. The exchange could be the result of the formation of maleic acid and the subsequent dehydration to maleic anhydride. Maleic anhydride combustion experiments (*46*) and *in situ* infrared spectroscopy studies (*48–49*) indicate that maleic acid is formed at low levels under these conditions. Incorporation of 5% ^{18}O is also observed for the 54 *m/e* fragment of maleic anhydride, which retains only terminal maleic anhydride oxygens (*50–51*). Thus, all maleic anhydride oxygen atoms undergo an equivalent exchange, adding justification to a mechanism which involves ring opening. To produce these ^{18}O levels in the effluent the additional oxygen required to form the maleic acid intermediate would have to be derived from a 20% ^{18}O pool. It is interesting to note that the furan produced from maleic anhydride contains relatively large amounts of ^{18}O. This indicates that the loss of oxygen must be extensive.

An overview of the reaction mechanism for *n*-butane conversion to maleic anhydride is provided in Fig. 4. Activation of the paraffin has been suggested by other workers to involve V=O sites, and the dehydrogenated C_4–hydrocarbon intermediate is proposed to be strongly adsorbed and constrained in such a manner that it reacts only at specific P–O–V sites. Further incorporation of oxygen occurs at sites also involving P–O–V bonding to produce maleic anhydride. In considering the routes to combustion products (CO_2 and H_2O), it is apparent that some maleic anhydride combustion occurs, but

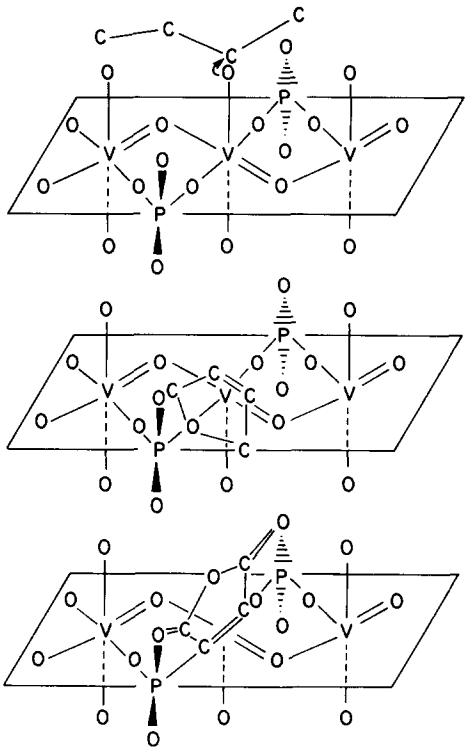

FIG. 4. Active site proposed for the conversion of *n*-butane to maleic anhydride.

mostly at V=O sites. However, nonselective oxidation products are also produced when highly reactive C_1–C_3 cracking products are formed at V=O sites, which are capable of reacting with all available lattice oxygen sites including the P–O–V sites involved in the insertion of oxygen to produce partially oxidized products. Thus, the selectivity of specific sites is dependent on the reactivity of the feed or intermediate. This is indicated by the interaction of 1-butene and 1,3-butadiene with different sites on the surface, even though maleic anhydride can also be produced from these feeds. It is also apparent from these studies that although adsorbed species formed from *n*-butane are likely partially dehydrogenated and even "furan-like," the fact that they are adsorbed makes their interaction with the surface quite different than that of gas-phase species. The conversion of *n*-butane to maleic

anhydride through these intermediates clearly would appear to involve specific interactions with only some P–O–V sites.

It should be pointed out that the techniques used in this research emphasize the reactivity of lattice (bulk) oxygen since no gas-phase oxygen was present. Other researchers (*23, 29–33*) have also addressed the importance of surface or adsorbed oxygen species. Under industrial reaction conditions, a more complex interaction involving several types of oxygen species is possible.

CONCLUSIONS

The techniques—referred to as IR-SM—used in this research have provided a valuable insight into the reaction of *n*-butane with β-$VOPO_4$. Selective and nonselective oxidation routes could be distinguished with clear evidence for additional routes to CO_2 rather than only the consecutive combustion of maleic anhydride. In addition, new information about the role of possible reaction intermediates has been obtained. *n*-Butane is adsorbed and acitivated on β-$VOPO_4$ in an irreversible and specific manner resulting in a highly constrained, partially dehydrogenated species. This species can then react with P–O–V sites to form a furan-like species. Further oxygen insertion at other P–O–V sites produces maleic anhydride, the majority of which then desorbs. Olefins and furan, in the form of gas-phase species, do not play a major role in this mechanism. γ-Butyrolactone is also not a likely intermediate.

The IR-SM technique is a potentially powerful method for studying catalytic selective oxidation reactions which involve lattice oxygen. In implementing this approach, the following requirements must be satisfied: (1) Incorporation of ^{18}O into the catalyst must be localized in specific sites. However, this must occur uniformly throughout the catalyst sample. (2) The isotopic label in the catalyst must be "located" spectroscopically or by other techniques. Laser Raman and infrared spectroscopies can be used to determine the location of ^{18}O in labeled β-$VOPO_4$. Other techniques have also been shown to be useful for other oxides (*36*). (3) The incorporation of the isotopic label into selective and nonselective oxidation products and possible intermediates must be monitored, typically by using an online mass spectrometer. Pulse-reactor studies are a particularly attractive approach, as demonstrated in this and other research, but in some cases, continuous flow experiments are also informative (*35*).

ACKNOWLEDGMENTS

This work was conducted through the Ames Laboratory, which is operated for the U.S. Department of Energy by Iowa State University under Contract W-7405-eng-82 with the U.S. Department of Energy. This research is supported by the Office of Basic Energy Sciences, Chemical Sciences Division.

REFERENCES

1. Bordes, E. *Catal. Today* **1,** 449 (1987).
2. Centi, G., Trifiro, F., Ebner, J. R., and Franchetti, V. M., *Chem. Rev.* **88,** 55 (1988).
3. Wenig, R. W., and Schrader, G. L., *Ind. Eng. Chem. Fundam.* **25,** 612 (1986).
4. Juan, L., Lashier, M. E., Schrader, G. L., and Gerstein, B. C., submitted for publication.
5. Centi, G., and Trifiro, F., *Catal. Today* **3,** 151 (1988).
6. Moser, T. P., and Schrader, G. L., *J. Catal.* **92,** 216 (1985).
7. Wenig, R. W., and Schrader, G. L., *J. Phys. Chem.* **90,** 6480 (1986).
8. Ostroushko, V. I., Kernos, Yu. D., and Ioffe, I. I., *Neftekhimiya,* **12,** (3), 95 (1972).
9. Morselli, L., Riva, A., Trifiro, F., and Emig. G., *Chim. Ind.* **60** (10), 791 (1978).
10. Ai, M., Bountry, P., and Montarnal, R., *Bull. Soc. Chim. France.* **8–9,** 2775 (1970).
11. Ai, M., *Bull. Chem. Soc. Japan* **43** (1), 3490 (1970).
12. Varma, R. L., and Saraf, D. N., *J. Catal.* **55,** 361 (1978).
13. Escardino, A., Sola, C., and Ruiz, F., *An. Quim.* **69,** 385 (1973).
14. Wohlfhart, K., and Hofmann, H., *Chem. Ing. Tech.* **52,** (10), 811 (1980).
15. Hodnett, B. K., Permanne, Ph., and Delmon, B., *Appl. Catal.* **6,** 231 (1983).
16. Wustneck, N., Wolf, H., and Seeboth, H., *React. Kinet. Catal. Lett.* **21** (4), 497 (1982).
17. Centi, G., Fornasari, G., and Trifiro, F., *J. Catal.* **89,** 44 (1984).
18. Hodnett, B. K., and Delmon, B., *Appl. Catal.* **15,** 141 (1985).

19. Centi, G., Manenti, I., Riva, A., and Trifiro, F., *Appl. Catal.* **9,** 177 (1984).
20. Morselli, L., Trifiro, F., and Urban, L., *J. Catal.* **75,** 112 (1982).
21. Ai, M., *J. Catal.* **67,** 110 (1981).
22. Kruchinin, Y. A., Mishchenko, Y. A., Nechiporuk, P. P., and Gel'bshtein, A. I., *Kinet. Katal.* **25** (2), 369 (1984).
23. Pepera, M. A., Callahan, J. L., Desmond, M. J., Milberger, E. C., Blum, P. R., and Bremer, N. J., *J. Amer. Chem. Soc.* **107,** 4883 (1985).
24. Szakacs, S., Wolf, H., Mink, G., Bertoti, I., Wustneck, N., Lucke, B., and Seeboth, H., *Catal. Today* **1,** 27 (1987).
25. Hodnett, B. K., and Delmon, B., *Ind. Eng. Chem. Fundam.* **23,** 465 (1984).
26. Martini, G., Trifiro, F., and Vaccari, A. *J. Phys. Chem.* **86,** 1573 (1982).
27. Cavani, F., Trifiro, F., and Vaccari, A., *in* "Adsorption and Catalysis on Oxide Surfaces" (M., Che and G. C. Bond, Eds.), p. 287. Elsevier, Amsterdam, 1985.
28. Zazhigalov, V. A., Zaitsev, Y. P., Belousov, V. M., Wustneck, N., and Wolf, H., *React. Kinet. Catal. Lett.* **24** (3–4), 375 (1984).
29. Gleaves, J. T., Ebner, J. R., and Kuechler, T. C., *Catal. Rev. Sci. Eng.* **30** (1), 49 (1988).
30. Kung, H. H., *Ind. Eng. Chem. Prod. Res. Dev.* **25,** 171 (1986).
31. Matsuura, I., *in* "Proceedings, Eighth International Congress on Catalysis, Berlin, 1984,"Vol. IV, p. 473. Dechema, Frankfurt au Main, 1984.
32. Haber, J., *in* "Proceedings, Eighth International Congress on Catalysis, Berlin, 1984," Vol. IV, p. 276. Dechema, Frankfurt au Main, 1984.
33. Fricke, R., Jerchekewitz, H. G., Lischke, G., and Ohlmann, G., *Z. Anorg. Allg. Chem.* **448,** 23 (1979).
34. Centi, G., and Trifiro, F., *J. Mol. Catal.* **35,** 255 (1986).
35. Lashier, M. E., Moser, T. P., and Schrader, G. L., *in* "Studies in Surface Science and Catalysis: New Developments in Selective Oxidation" (G. Centi and F. Trifiro, Eds.), p. 573. Elsevier, Amsterdam, 1990.
36. Lashier, M. E., Ph.D. thesis, Iowa State University, 1989.
37. Gopal, R., and Calvo, Ca., *J. Solid State Chem.* **5,** 432 (1972).
38. Moser, T. P., and Schrader, G. L., *J. Catal.* **104,** 99 (1987).
39. Bordes, E., Johnson, J. W., Raminosona, A., and Courtine, P., *Mater. Sci. Monogr.* **28B,** 887 (1985).
40. Bhargava, R. N., and Condrate, R. A., Sr., *Appl. Spectrosc.* **31,** 320 (1977).
41. Tarte, P., *Acta Crystallogr.* **16,** 228 (1963).
42. Ross, S. D., "Inorganic Infrared and Raman Spectra." McGraw–Hill, New York, 1972.
43. Turell, G., "Infrared and Raman Spectra of Crystals." Academic Press, New York, 1972.
44. Nakamoto, K., "Infrared and Raman Spectra of Inorganic and Coordination Compounds," Wiley, New York, 1978.
45. Wilkinson, G. R., Raman spectra of ionic, covalent and metallic crystals, *in* "The Raman Effect" (A. Anderson, Ed.), Vol. 2. Dekker, New York, 1973.
46. Moser, T. P., Wenig, R. W., and Schrader, G. L., *Appl. Catal.* **34,** 39 (1987).
47. Garbassi, F., Bart, B., Tassinari, R., Vlaic, G., and Lagarde, P., *J. Catal.* **98,** 317 (1986).
48. Wenig, R. W., and Schrader, G. L., *J. Phys. Chem.* **91** (1), 1911 (1987).
49. Wenig, R. W., and Schrader, G. L., *J. Phys. Chem.* **91** (22), 5674 (1987).
50. Stenhagen, E., Abrahamson, S., and McLafferty, F. W. (Eds.), "Atlas of Mass Spectral Data", Interscience, New York, 1969.
51. Lashier, M. E., and Schrader, G. L., to be published.